

Towards FSI: LDA-Investigations of the Flow past a Hemisphere in an Artificially Generated Turbulent Boundary Layer

LDA-Messungen zur Umströmung einer starren Halbkugel in einer künstlich erzeugten Grenzschicht als Grundlage für Untersuchungen zur Fluid-Struktur Interaktion

J. N. Wood, M. Breuer

Professur für Strömungsmechanik, Helmut-Schmidt-Universität Hamburg, D-22043 Hamburg

hemisphere; turbulent flow; laser-Doppler anemometry; artificial boundary layer;
Halbkugel; turbulente Strömung; Laser-Doppler Anemometrie; künstliche Grenzschicht.

Abstract

The present study investigates the complex flow field around a surface-mounted smooth hemisphere (presently rigid) within a turbulent boundary layer at a Reynolds number of $Re = 50,000$ based on the diameter D of the model and the free-stream mean velocity. Special emphasis is put on the artificial boundary layer thickening techniques that are applied to mimic the influence of a fully developed turbulent boundary layer as inflow condition. A presentation of the applied devices outlines the possibility to achieve the desired boundary layer thickness of $\delta = D/2$ within a geometrically restricted experimental setup. The measurements are conducted in a wind tunnel using laser-Doppler anemometry to measure the velocity field around the hemisphere in the symmetry plane. A detailed analysis of the flow characteristics such as the horseshoe vortex system and the recirculation area is carried out. However, the main motivation for the present study is to extend the experimental investigations towards fluid-structure interaction. For this purpose, a flexible thin-walled membraneous structure of hemispherical shape is planned to be exposed to the turbulent flow. Besides the flow measurements the deformations and the fluctuations of the air-inflated structure will be measured based on a digital-image correlation technique. The long-term goal of this study is to provide detailed measurements of the flow field and the structure deformation, which can be used as a benchmark case for coupled FSI simulations.

Introduction

Flow fields around surface-mounted bluff bodies in turbulent boundary layers are of common interest in environmental and civil engineering. Spherically shaped objects such as domed structures exhibit very complex flow patterns that can be roughly classified into an upstream horseshoe vortex system and a recirculation area with trailing vortices in the wake region. The present study focuses on the experimental investigation of the flow field around a surface-mounted smooth hemisphere in a turbulent boundary layer using the laser-Doppler measurement technique. The flow field of the hemisphere has been investigated intensively in a series of publications such as Toy et al. (1983), Savory and Toy (1986) and Savory and Toy (1988). However, the motivation for the present experiment is to establish a starting point for the preceding studies of a thin-walled, flexible membraneous structure that is used to

carry out fluid-structure interaction (FSI) measurements. However, within a preliminary study an appropriate setup has to be found under the restrictions of the given localities that assures reproducible results. For this purpose, a rigid hemisphere is chosen as a meaningful model to gain information about the flow field as initial conditions for the FSI studies. Furthermore, the oncoming flow shall mimic the character of a fully developed boundary layer which thickness matches the height of the hemisphere. This is only possible by generating an artificially thickened boundary layer to overcome the problem of the restricted dimensions of the test section. The results are also used to validate a complex three-dimensional large-eddy simulation which is performed in parallel. The long-term objective of the present studies is to utilize the experimentally gained data as a reference to validate coupled FSI simulations of thin-walled structures exposed to turbulent flow conditions. A preliminary experimental examination of a flexible hemisphere suggests a promising possibility to advance the studies towards FSI.

Description of the case

A rigid hemisphere (diameter D) is mounted on a smooth wall as depicted in Fig. 1. The surface of the hemisphere is considered to be ideally smooth. The structure is put into a thick turbulent boundary layer which can be described by a 1/7 power law as reviewed by Counihan (1975). At a distance of $1.5 D$ upstream of the dome the thickness of the boundary layer δ corresponds to the height of the hemisphere, i.e., $\delta = D/2$. The Reynolds number of the air flow ($\rho = 1.225 \text{ kg/m}^3$, $\mu = 18.27 \times 10^{-6} \text{ kg/(m s)}$ at $\theta = 20^\circ\text{C}$) is set to about $\text{Re} = \rho U_\infty D / \mu \approx 50,000$. U_∞ is the free-stream mean velocity in x -direction outside the boundary layer at standard atmospheric conditions. The Mach number is low ($\text{Ma} < 0.03$). At this Mach number the air flow can be assumed to be incompressible. Moreover, the fluid is considered to be isotherm. In the present paper all quantities are given in dimensionless form using the diameter of the dome D , the free-stream velocity U_∞ and the fluid density ρ . The origin of the frame of reference is taken at the center of the base area of the hemisphere, where x denotes the streamwise, y the spanwise and z the vertical (wall-normal) direction.

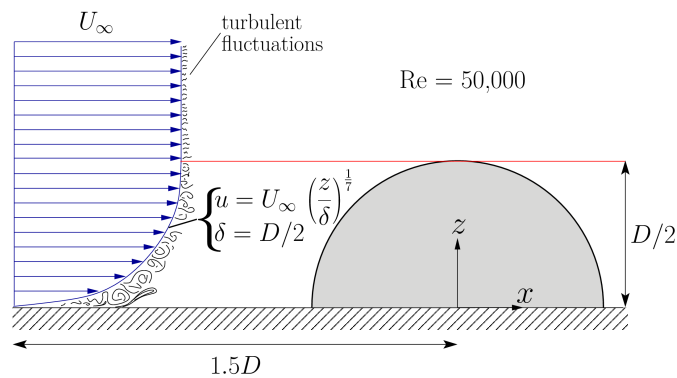


Fig. 1: Surface-mounted hemisphere within a turbulent boundary layer.

Experimental setup

The experimental investigations for the flow past the hemisphere are carried out in a Göttingen-type subsonic wind tunnel with an open test section. The hemisphere is placed on a flat smooth plate which is mounted onto a table adjustable in height. The dimensions and the position of the model in the test section are illustrated in Fig. 2 with reference to the symmetry plane of the setup. The flat plate is designed to cover the complete spanwise extension of the cross-section of the wind tunnel in order to ensure a smooth transition of the near-wall

flow from the nozzle to the test section. The model of the hemisphere as well as the flat plate are made of aluminum for low manufacturing tolerance and smooth surfaces.

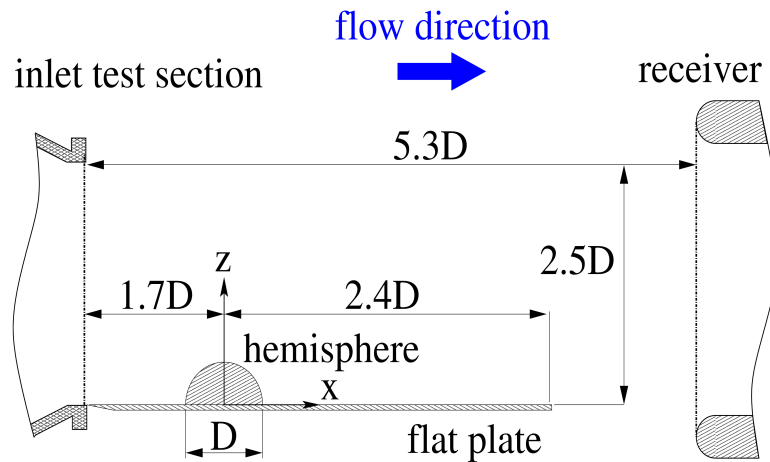


Fig. 2: Illustration of the dimensions of the test section based on the diameter of the hemisphere.

The diameter of the hemisphere is $D = 150$ mm. The blocking ratio of the hemisphere in the wind tunnel is approximately 4.7% based on the projected area $A_{\text{hemi}} = \pi/8 D^2$ of the hemisphere and the area of the cross-section of the nozzle. To adjust the Reynolds number to $Re = 50,000$, the blower of the wind tunnel is operated at a free-stream velocity $U_\infty = 5.14$ m/s. For an empty test section without any artificial boundary layer thickening technique the free-stream streamwise turbulence intensity of the wind tunnel is $Tu_u = u'_{\text{rms}}/U_\infty < 0.2\%$.

The flow past the hemisphere is measured by a non-invasive 2-D laser-Doppler anemometer offering high resolution velocity measurements of the streamwise and wall-normal components, u and w , respectively. The laser beam is generated by a water-cooled Coherent Innova 70C argon-ion laser. The beam is guided to a Dantec FiberFlow transmitter box, where it is split up into two different wave lengths (514.5 nm and 488 nm) which are used for each velocity component. The beams are sent from the transmitter box to a 2-D optical probe. A traverse with three translational degrees of freedom is carrying the optics. The measurement of the wall-normal component w is geometrically restricted by the crossing angle of the laser beams. When the probe moves closer to the surface, a certain position is reached (i.e. 13 mm above the surface) where the lower laser beam hits the edge of the flat plate and is blocked. Thus, in the near-wall region the flat plate acts as an optical barrier that interrupts the formation of the measuring volume. Consequently, no data can be recorded for the wall-normal component below this particular point. The measurements and the positioning of the traverse are operated by the Dantec BSA Flow Software. The measuring plane of the LDA setup focuses on the symmetry plane of the flow field and is given in Fig. 3.

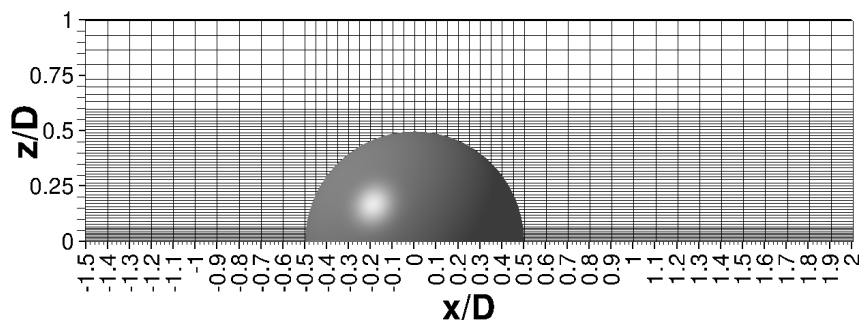


Fig. 3: Grid resolution of the measurement containing 2041 measurement points.

The chosen plane ranges from $-1.5 < x/D < 2$ in streamwise and from $0 < z/D < 1$ in vertical direction. The utilized grid of measurements contains 2041 measurement points composed of 46 velocity profiles along the streamwise extension. Each profile contains 57 points in wall-normal direction with exceptions for the locations close to the hemisphere. Local refinement is applied in the vicinity of the hemisphere and the near-wall region to ensure an appropriate gradient resolution. This is especially necessary for the expected shear layer distribution in the wake regime and the horseshoe vortex in front of the hemisphere close to the plate.

Generation of the artificially thickened boundary layer

The development of the turbulent boundary layer on the flat plate (without placing the model of the hemisphere in the test section) is investigated by analyzing the influence of common turbulence generators (Lawson, 1968; Counihan, 1969; Sargison et al., 2004).

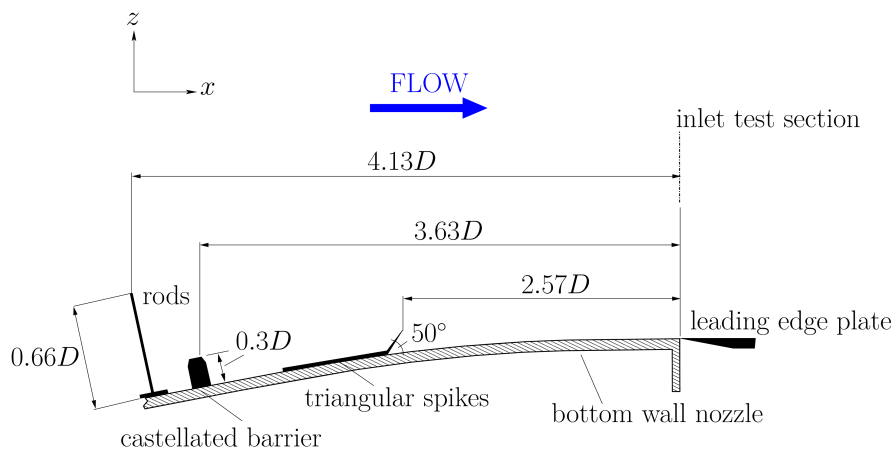


Fig. 4: Setup of the turbulence generators in the nozzle of the wind tunnel.

Due to the restricted dimensions of the test section the possible location of the devices is geometrically limited. The challenge of artificial boundary layer design is the generation of thick boundary layers over relatively short distances. Artificially high turbulence intensities that occur from using inappropriate devices must be avoided to achieve similar results compared to a naturally developing boundary layer. An intensive study of several turbulence generator leads to the optimum combination of these devices to achieve the desired boundary layer profile within the given working space. As a final outcome a fence with equidistant rods followed by a castellated barrier and a fence with triangular spikes is chosen to mimic the development of a natural turbulent boundary layer over a long distance. A schematic representation of the setup is depicted in Fig. 4. To check the outcome velocity data are recorded just after the beginning of the test section at $x/D = -1.5$ in the symmetry plane without placing the hemisphere into the test section. As a reference velocity distribution the 1/7 power law with $\delta = D/2$ is used to evaluate the measurements. The power law is illustrated in Fig. 5 as a continuous line and the LDA measurements are given as symbols. The measured mean velocity distribution u/U_∞ is in close agreement with the reference exhibiting minor deviations in the region $z/D = 0.25$. The free-stream velocity $u/U_\infty \approx 1$ is reached at about $z/D \approx 0.5$ which indicates that the desired thickness of the boundary layer is attained. Additionally, the displacement thickness δ_1/δ and the momentum thickness δ_2/δ are evaluated from the experimental data to $1/8$ and $7/72$, respectively. It leads to a shape factor of $H = \delta_1/\delta_2 = 1.286$ which confirms a classical property of a turbulent boundary layer. The Reynolds number based on δ_2 is estimated to $Re_{\delta_2} = 2503$. The turbulent fluctuations u'_{rms}/U_∞ and w'_{rms}/U_∞ are given in percent of the free-stream velocity. Similar distributions were obtained by Schlatter et al. (2009) based

on a direct numerical simulation (DNS) of a turbulent boundary layer flow on a flat plate with smooth surface at a Reynolds number of $Re_{\delta_2} = 2500$.

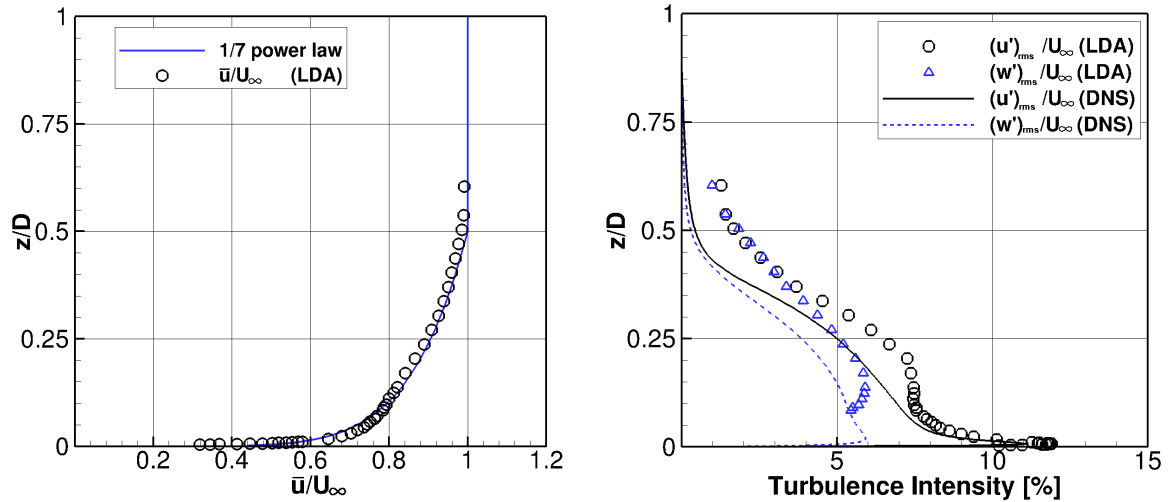


Fig. 5: Inflow properties of the turbulent boundary layer at the inlet of the test section. The distribution of turbulent intensity is compared to the DNS results of Schlatter et al. (2009).

The streamwise turbulent fluctuations u'_{rms}/U_{∞} gradually increase from the free-stream (1.2%) to the near-wall region with a peak value of about 12.1% at $z/D = 0.01$.

The measurements of the turbulent boundary layer is independently conducted from the previously mentioned measurement grid of the actual hemisphere setup. Moreover, the additional measurements comprise a high spatial resolution of the near-wall region. These data are of general interest for the complementary numerical investigations based on the large-eddy simulation technique where the experimental properties of the boundary layer flow are used as reference data to generate comparable inflow conditions.

Time-averaged results and discussion

This section presents the time-averaged results of the flow around the hemisphere. The outlined approach using 2-D color plots offers the possibility to identify characteristic regions that are introduced and discussed in numerous publications (Savory and Toy, 1986; Savory and Toy, 1988). The key aspects focus on the detailed view of the velocity field and the associated Reynolds stresses in the symmetry plane.

The streamwise and wall-normal velocity components are given in Fig. 6. The experimental results show that the thickness of the approaching boundary layer is matching the height of the hemisphere well with $z/D \approx 0.5$. The development of a recirculation area close to the plate can be observed in front of the hemisphere between $-0.75 < x/D < -0.5$. This phenomenon is connected to the horseshoe vortex. It results from the reorganization of the approaching boundary layer which detaches from the ground at $x/D = -0.8$ due to the positive pressure gradient (stagnation area) located in front of the hemisphere. The size of the horseshoe vortex depends on the turbulence intensity of the approaching flow. The next distinct location is the separation point where the flow detaches from the surface of the hemisphere. It marks an important characteristic for the validation of numerical simulations since its position depends on multiple physical flow properties such as the Reynolds number, the turbulence intensity of the boundary layer and the surface roughness. After exceeding the separation point the flow detaches from the surface of the hemisphere which leads to the development of a free shear layer. This phenomenon can be observed as a strong velocity gradient between the outer

flow field and the recirculation area in the wake flow. The size of the recirculation area stretches up to $x/D \approx 1$ and is interrelated to the turbulence intensity of the approaching boundary layer. According to previous studies (Toy et al., 1983; Savory and Toy, 1988; Tavakol et al., 2010; Kharoua and Khezzer, 2013) the turbulence level of the oncoming flow influences the length of the recirculation area since for an increasing level the location of the separation point is shifted towards a further downstream position on the hemisphere. The flow finally reattaches at about $x/D = 1.04$.

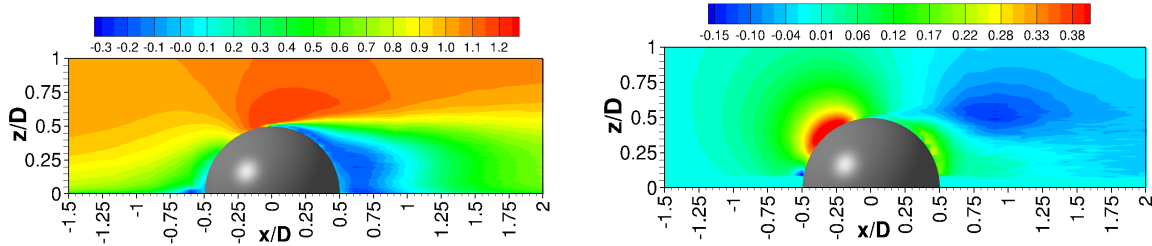


Fig. 6: Time-averaged velocity components in the symmetry x - z -plane at $y/D=0$.

The wall-normal velocity component \bar{w}/U_∞ close to the bottom wall in the region $0 < z/D < 0.08$ is not resolved in the experimental investigation due to the restrictions of the test setup mentioned in “Experimental setup”. A notable region is the area of increasing \bar{w} velocity component at the front side of the hemisphere at $-0.45 < x/D < -0.15$ and $0.25 < z/D < 0.45$ resulting from the acceleration of the fluid after exceeding the stagnation area.

Fig. 7 refers to the normal Reynolds stresses $\overline{u'u'}/U_\infty^2$ and $\overline{w'w'}/U_\infty^2$, respectively. The highest Reynolds stresses appear in the free shear layer right after the separation point due to the rapid roll-up process of the vortical structures. This region stretches out into the upper recirculation region where turbulent mixing is perceived. Also the oscillating movement of the recirculation area, related to large vortical structures that detach from the hemisphere, contributes to the perceived Reynolds stresses.

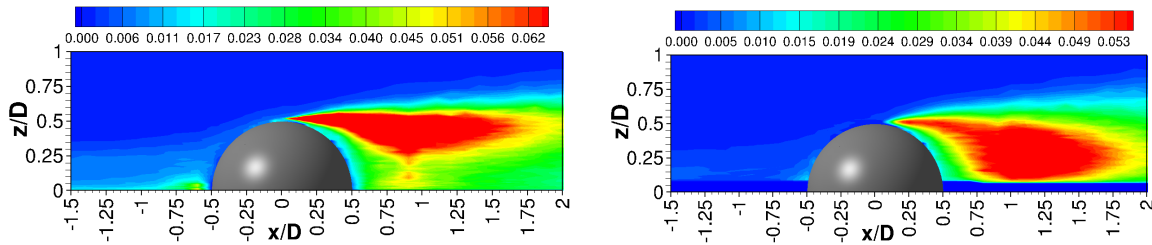


Fig. 7: Normal Reynolds stress components $\overline{u'u'}/U_\infty^2$ and $\overline{w'w'}/U_\infty^2$ in the symmetry x - z -plane at $y/D=0$.

Steps towards FSI

A preliminary study is currently examining possible manufacturing techniques to obtain a thin-walled flexible structure that represents a smooth hemisphere in a best way. The thickness of the wall has to be small compared to its overall dimensions to obtain membraneous properties suitable for the desired model used in fluid-structure interaction investigations. A membraneous character of the model is considered to be ideal to mimic an air-inflated structure which is exposed to a turbulent boundary layer and is deformed by the wind load.

At present a two-component silicon rubber is used in a casting process to shape the contour of a thin and hollow hemisphere. The dimensions of the hemisphere are identical to the rigid test case to maintain the geometrical conditions. Quality tests are conducted to analyze the reproducibility of the manufacturing process. Furthermore, the deformation behavior of the chosen silicon material is examined. A customized test setup is designed in which the hollow

hemisphere is fixed to a plate with a circular cutting which offers access to the bottom side of the plate. A pressure valve is connected to the lower side of the plate in order to stabilize the contour of the hemisphere by applying a slight gauge pressure.

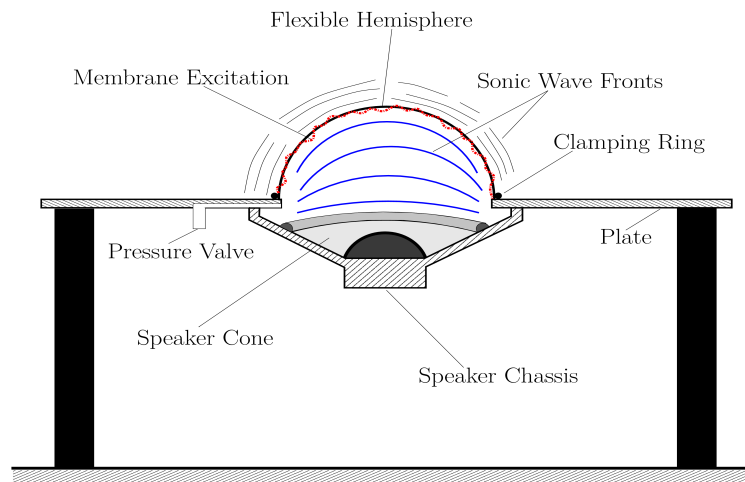


Fig. 8: Test setup used to validate the behavior and the properties of the flexible hemisphere.

A loud speaker is mounted to the reverse side of the plate. Its cone points towards the inner contour of the pressurized hemisphere. The speaker is used to produce specific waves of predefined frequencies with large amplitudes to force controlled excitations of the hemisphere as schematically presented in Fig. 8.

A digital-image correlation system consisting of two high-speed cameras is applied to capture the dynamic response of the flexible hemisphere while the loud speaker is active. The stochastic dot pattern on the outer contour of the hemisphere is mandatory for the correlation algorithm to evaluate the deformations. During the evaluation process every time step of the high-speed measurement is represented by two pictures, one for each camera. Every time step can be considered as an image pair showing the deformed structure from different view points to gather efficiently three-dimensional information. Each image pair contains a certain overlapping area in which both pictures show an identical dot pattern. This area is closely connected to the chosen camera setup (angle between both cameras, distance to the model) and determines the region of data evaluation. Typically a specific dot within the overlapping region is selected in a reference image as an initial starting point for the evaluation. The software verifies the chosen dot in each image pair referring to the reference. If the procedure is successful the correlation algorithm searches for homologous dots in the entire overlapping area to perform the deformation analysis. After the evaluation run has finished a suitable reference configuration (undeformed structure on the left) is necessary in order to calculate the deformation at each time step.

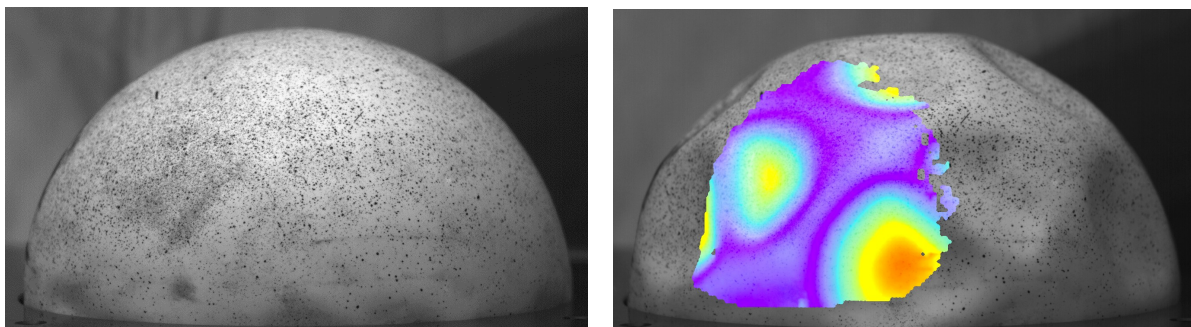


Fig. 9: Undeformed reference configuration (left) and excited hemisphere (right). The colored area represents the total displacements (in mm) within the overlapping area.

A snapshot of an arbitrary moment of the deformed structure of the hemisphere compared to the non-deformed static state is shown in Fig. 9. This particular test was conducted with a speaker frequency of $f = 40$ Hz. Large regular deformations are observable along the contour of the excited hemisphere which show the response of the structure to the periodic excitation by the loud speaker. The colored area indicates the total displacements (in mm) referring to the reference configuration. In a further step the flexible hemisphere shall be transferred into the wind tunnel to conduct fluid-structure interaction experiments in a turbulent boundary layer. Complementary particle-image-velocimetry measurements are planned to determine the flow field during the interaction between the flow and the flexible hemisphere.

Conclusions

Laser-Doppler anemometry is utilized to analyze the velocity field and the associated Reynolds stresses of the flow past a surface-mounted rigid hemisphere in a wind tunnel exposed to an artificially generated turbulent boundary layer. An optimized setup of turbulence generators is capable to mimic the characteristics of a naturally developing boundary layer in a reproducible manner. The collected data of the rigid hemisphere shall be used in a twofold manner: On the one hand they represent the starting point for the following measuring campaign which comprises a thin-walled flexible hemisphere for investigations of fluid-structure interaction of membraneous structures. On the other hand the experimentally determined data are the basis for the validation of the complementary LES predictions.

References

- Counihan, J., 1969: "An improved method of simulating an atmospheric boundary layer in a wind tunnel", *Atmospheric Environment* 3, pp. 197-214
- Counihan, J., 1975: "Adiabatic atmospheric boundary layers: a review and analysis of data from the period 1880-1972", *Atmospheric Environment* 9, pp. 871-905
- Kharoua, N., Khezzar, L., "Large-eddy simulation study of turbulent flow around smooth and rough domes", *Proceedings of the Institution of Mechanical Engineers, Part C: Journal of Mechanical Engineering Science* 227 (12), pp. 2686-2700
- Lawson, T. V., 1968: "Methods of producing velocity profiles in wind tunnels", *Atmospheric Environment* 2, pp. 73-76
- Sargison, J. E., Walker, G. J., Bond, V., Chevalier, G., 2004: "Experimental review of devices to artificially thicken wind tunnel boundary layer" in: M. Behina, W. Lin, G.D. MaBain (Eds.), *Proceedings of the Fifteenth Australian Fluid Mechanics Conference (CD-ROM)*, The University of Sydney, AFMC00091
- Savory, E., Toy, N., 1986: "Hemisphere and hemispherical-cylinders in turbulent boundary layers", *Journal of Wind Engineering and Industrial Aerodynamics* 23, pp. 345-364
- Savory, E., Toy, N., 1988: "The separated shear layers associated with hemispherical bodies in turbulent boundary layers", *Journal of Wind Engineering and Industrial Aerodynamics* 28, pp. 291-300
- Schlatter, R., Orlu, R., Li, Q., Brethouwer G., Fransson, J. H. M., Johanesson, A. V., Alfredsson, P. H., Henningson, D. S., 2009: "Turbulent boundary layers up to $Re_\theta = 2500$ studied through simulation and experiment" *Physics of Fluids* 21 (051702), pp. 1-4.
- Tavakol, M. M., Yaghoubi, M., Masoudi Motlagh, M., 2010: "Air flow aerodynamic on a wall-mounted hemisphere for various turbulent boundary layers", *Experimental Thermal and Fluid Sciences* 34 (5), pp. 538-553
- Toy, N., Moss, D., Savory, E., 1983: "Wind tunnel studies on a dome in turbulent boundary layers", *Journal of Wind Engineering and Industrial Aerodynamics* 11, pp. 201-212